

# OPTICAL SCIENCES CENTER

University of Arizona

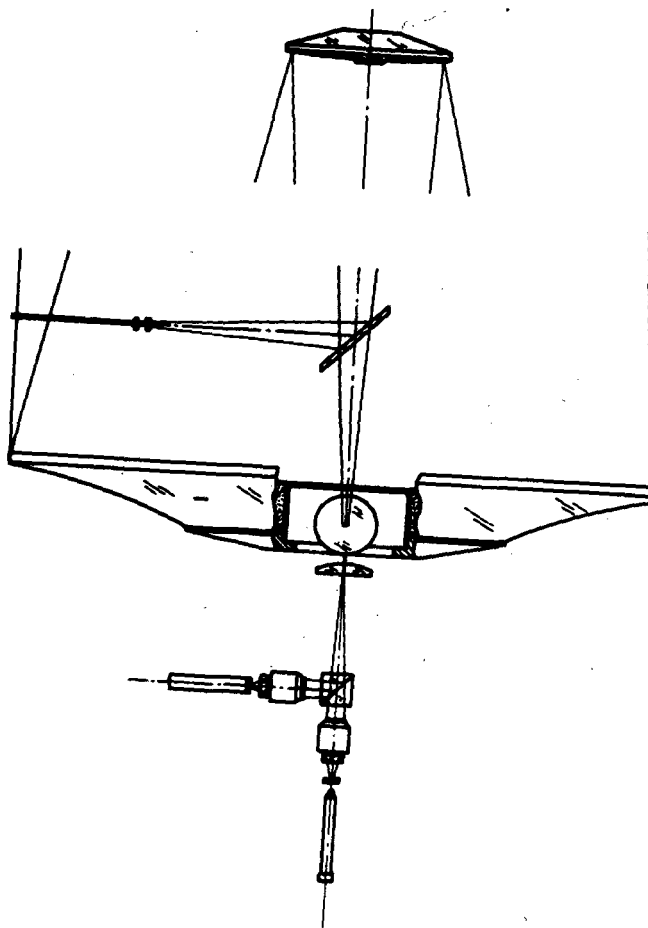
(NASA-CR-139486) THE DESIGN, CONSTRUCTION  
AND TESTING OF THE OPTICS FOR A  
147-CM-APERTURE TELESCOPE (Arizona Univ.,  
Tucson.) 30 p HC \$4.50 - CSCI 20F

G3/14 45952

Unclass

N74-30898

*Super AD-756 746*



*The Design, Construction, and Testing of  
the Optics for a 147-cm-Aperture Telescope*

*R. A. Buchroeder, L. H. Elmore, R. V. Shack, and P. N. Slater*

TECHNICAL REPORT 79

DEC. 1972

## ABSTRACT

In this report we describe the work carried out under contract F19628-72-C-0047 entitled "Geodetic Optics Research" for the Air Force Cambridge Research Laboratories (AFCRL). The work consisted mainly of the fabrication of the optical components for a telescope with a 152-cm-diam (60-in.) primary mirror masked down to 147-cm diam for use by the AFCRL for a lunar ranging experiment.

Among the noteworthy achievements of this contract were the following:

(a) Completion of the primary and secondary mirrors for a high-quality 147-cm-diam telescope system in eight months from the start of edging the primary.

(b) Manufacture and testing of a unique center mount for the primary according to an AFCRL design that allowed for a thin-edged and therefore less-massive mirror.

(c) Development of a quantitative analysis of the wire test for calculating the departure of the mirror figure from the design figure quickly and accurately after each polishing step. This analysis method in conjunction with a knowledge of polishing rates for given weights and diameters of tools, mirror, and polishing materials should considerably reduce the polishing time required for future large mirrors.

The emphasis in this report is on these three items; however, considerable work was also undertaken in telescope design; null lens design and mounting; tracking optics design, fabrication, and mounting; and special thin-film coatings for the laser send and receive optics.

THE DESIGN, CONSTRUCTION,  
AND TESTING OF THE OPTICS FOR  
A 147-CM-APERTURE TELESCOPE

*R. A. Buchroeder, L. H. Elmore, R. V. Shack, and P. N. Slater*

*Optical Sciences Center, University of Arizona, Tucson, Arizona 85721  
Technical Report 79, December 1972*

CONTENTS

INTRODUCTION . . . . . 1

SYSTEM SPECIFICATIONS . . . . . 3

    Telescope Optics . . . . . 3

    Tracker Optics . . . . . 3

PROGRAM SCHEDULE AND LOG OF FABRICATION

    OF PRIMARY MIRROR . . . . . 4

        Lunar Laser Telescope Schedule Plan . . . . . 5

        Log of Fabrication . . . . . 7

PRIMARY MIRROR BLANK SHAPE AND MOUNT DESIGN . . . . . 10

OPTICAL DESIGN . . . . . 12

    Telescope Optics . . . . . 12

    Test Optics . . . . . 13

    Laser Channel . . . . . 13

    Tracker Optics . . . . . 14

    Further Design Considerations . . . . . 15

QUANTITATIVE WIRE TEST ANALYSIS . . . . . 18

    Theory . . . . . 18

    Application . . . . . 20

OPERATIONAL TEST RESULTS . . . . . 24

REFERENCES . . . . . 26

## INTRODUCTION

Since the emplacement of retroreflectors on the lunar surface by astronauts in July 1969, several groups of scientists have been conducting lunar laser ranging experiments from different observatories in this and other countries. The results of such experiments are of considerable importance to both lunar and geodetic scientists. One such group, from the Air Force Cambridge Research Laboratories (AFCRL), headed by M. S. Hunt and including W. E. Carter, the contract monitor for the work described here, was stationed in Tucson, Arizona, and used observing sites in the Catalina Mountains.

In their early attempts at lunar ranging, they used a 152-cm (60-in.) aperture metal mirror telescope of the inverted Dall-Kirkham design (spherical primary mirror and elliptical secondary mirror). They used different metal primary mirrors, all of which proved unsuited for their experiment. For example, the best system they tried had an initial blur image diameter of about 5 arc sec immediately after fabrication and installation, which deteriorated and stabilized to about 10 arc sec after several weeks. A second problem encountered by Hunt's group was that the useful field of an inverted Dall-Kirkham telescope is too restricted to allow for main-field tracking. This meant that an auxiliary tracking telescope had to be used. Unfortunately, it did not remain sufficiently well boresighted with the main telescope when the latter was slewed.

At a meeting in the Optical Sciences Center in March 1971 between members of the University of Arizona and the AFCRL it was resolved that the gift of a 183-cm-diam (72-in.) CER-VIT mirror by Dr. A. B. Meinel, Director, Optical Sciences Center, to the AFCRL would enable a completely new optical system to be designed, fabricated, and mounted in the existing telescope fixtures without exceeding AFCRL's time budget for the lunar laser ranging experiment. In this report we describe the work carried out under contract F19628-72-C-0047 entitled "Geodetic Optics Research" for the Air Force Cambridge Research Laboratories (AFCRL). The work consisted mainly of the fabrication of the optical components for a telescope with a 152-cm-diam (60-in.) primary mirror masked down to 147-cm diam for use by the AFCRL for a lunar ranging experiment.

Many of the staff of the Optical Sciences Center made substantial contributions to the program. A list of their names and activities follows:

J. C. Bailey	Coordinator
C. N. Brown	Machinist
R. A. Buchroeder	Optical designer
C. W. Burkhardt	Chief machinist
L. H. Elmore	Primary mirror fabricator
D. A. Loomis	Chief optician
A. B. Meinel	Consultant
J. Poulos	Thin film coater
R. V. Shack	Testing consultant
P. N. Slater	Principal investigator
R. E. Sumner	Tracker and null optics fabricator
R. H. Tornquist	Mechanical designer

In addition, the personal day-to-day involvement of W. E. Carter, M. S. Hunt, and W. G. Robinson (AFCRL) was most helpful in the problem of integrating components fabricated at the Optical Sciences Center with the existing AFCRL telescope fixtures.

## SYSTEM SPECIFICATIONS

The specifications for the contract can be divided into two parts: telescope optics and tracker optics. In fact, considerably more items than these were involved in the project (see, for example, the next section), but telescope and tracker optics fabrication and testing were the most critical parts of this contract. Items covered prior to actual contract commencement are reported for program continuity but were funded from other sources.

### *Telescope Optics*

The components were to be designed and fabricated to interface with the existing fixtures of the AFCRL telescope and to meet the following specifications:

Primary mirror: 152-cm (60-in.) diam,  $f/2.5$ , CER-VIT

Secondary mirror: 41-cm (16-in.) diam, final speed  $f/8$ , CER-VIT

Over-all system:  $f/8$ , Ritchey-Chrétien design, 15 arc min semifield angle

System performance on axis: 80% of total energy from a point source to fall within a 2 arc-sec-diam circle for a semifield angle of 3 arc min; 80% of total energy from a point source to fall within a 4-to 5 arc-sec-diam circle for field angles from 3 arc min to 15 arc min.

### *Tracker Optics*

The following were to be designed and fabricated to interface with existing fixtures of the AFCRL telescope:

Laser beamsplitter

Field lenses

Transfer optics

Field flatteners

Optical-mechanical mounts

Tracker housing

Other interfacing components

When fabricated and installed, these were to meet the specifications called for above for system performance off axis.

## PROGRAM SCHEDULE AND LOG OF FABRICATION OF PRIMARY MIRROR

The schedule plan for the work for the AFCRL is shown on pages 5 and 6, and photographs of the work are shown on pages 8 and 9. Not every item was finished on schedule, but there were nearly as many finished ahead of, as behind, schedule. No item was critically behind the planned schedule shown; minor discrepancies may be found between the Lunar Laser Telescope Schedule Plan and related parts of the Log of Fabrication shown on page 7.

The fabrication log should be of value to those estimating the time to allow for fabricating a high-quality mirror of 152-cm diam. However, it should be noted that this log will be a guide only for low-expansion materials such as Owens-Illinois' CER-VIT and Corning's ULE silica. Higher expansion materials will take significantly longer owing to the time required for the mirror to come to thermal equilibrium after polishing and cleaning. For example, with the CER-VIT blank it was possible to perform 1 h of polishing followed by 1 h of testing several times a day during the final days of polishing.

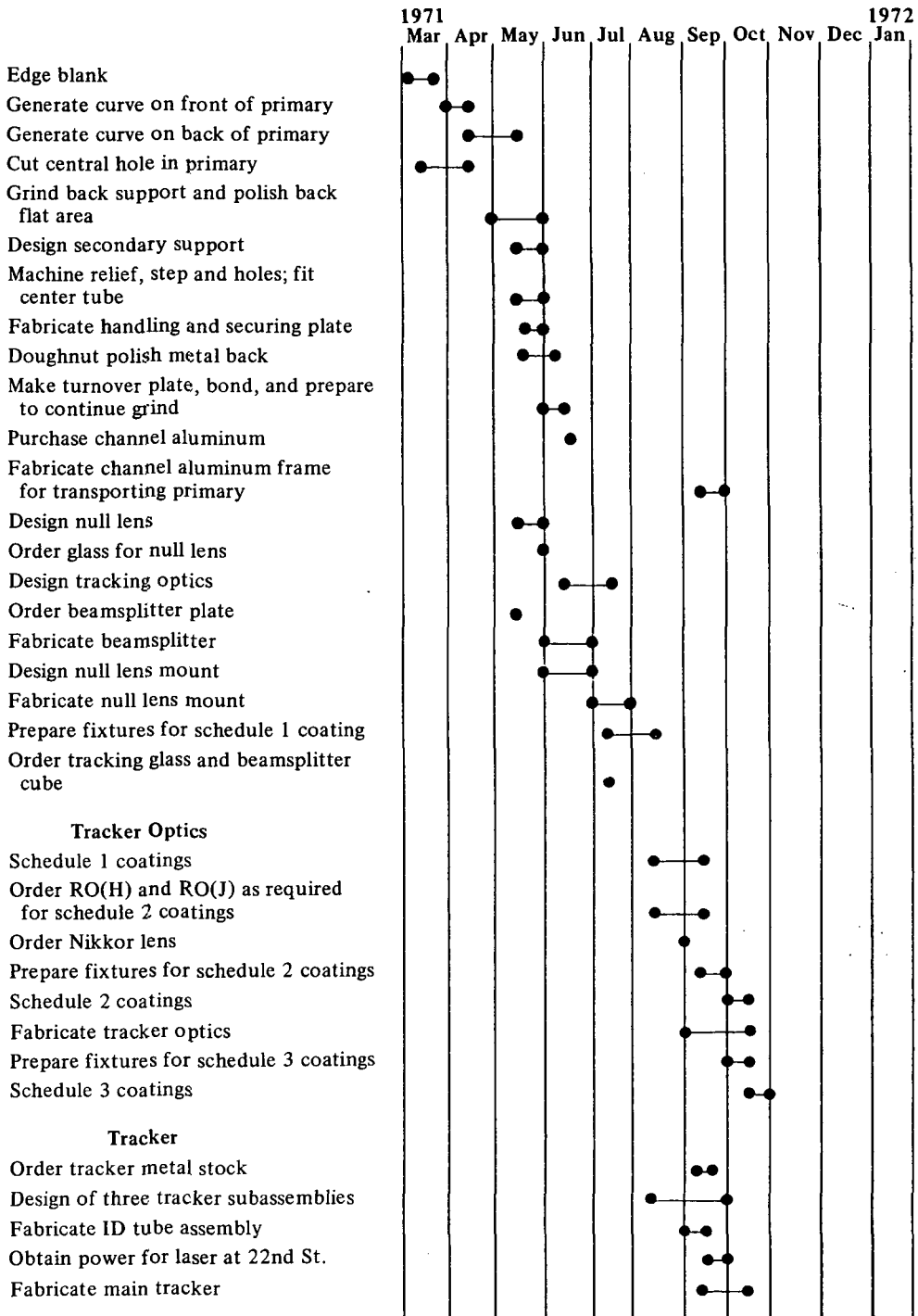
It will be of interest to those concerned with detailed scheduling that the following time was spent polishing the 152-cm-diam primary:

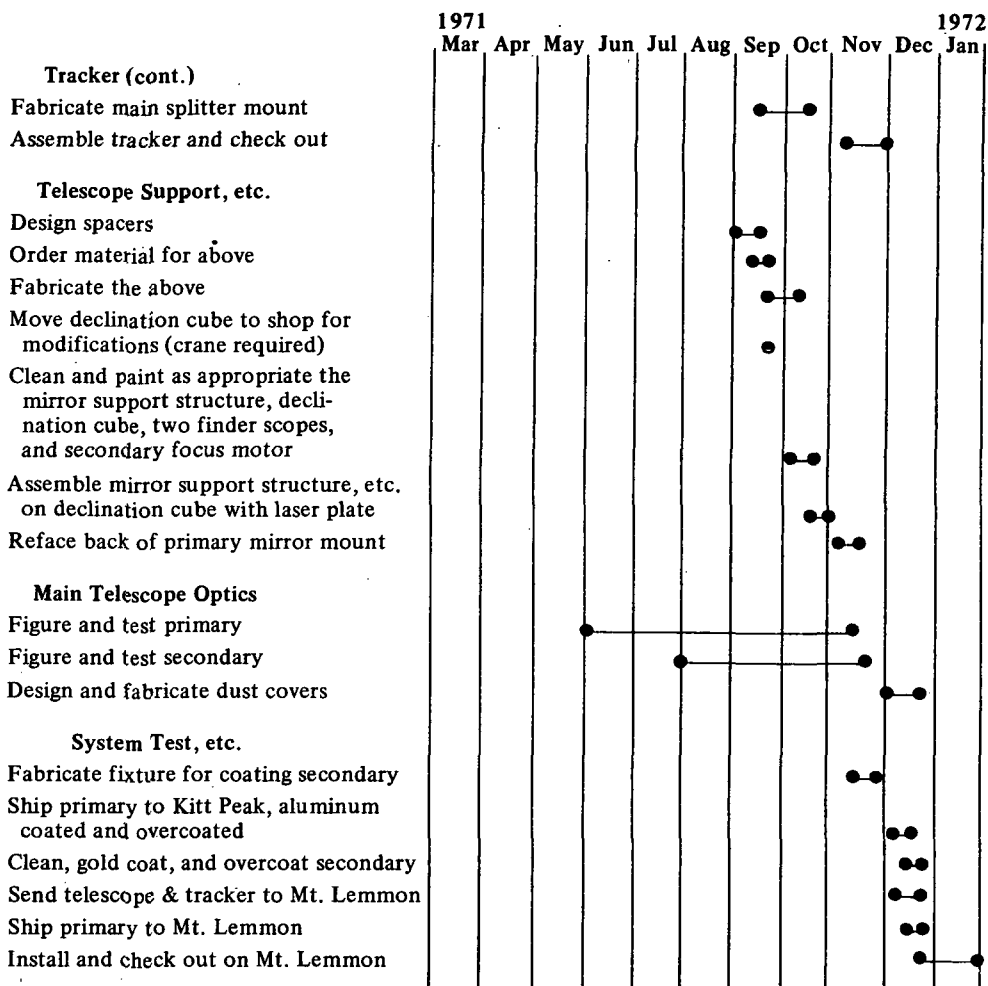
June	11 days
July	21 days
August	22 days
September	21 days
October	7 days
TOTAL	82 days

At 8 h per day this amounts to 656 h, which were divided into 380 h of polishing time, 260 h of cleaning, trimming laps, and testing, and 16 h of machine repair time. The bulk of the polishing time was spent with one man at the machine, which was run without stopping during the day, thereby saving approximately 2 h of preparation time per day; usually several men were involved in testing the mirror.



**Lunar Laser Telescope Schedule Plan  
(March 1971 through January 1972)**





In addition, checking and analysis of the telescope, the electronic systems, and the site support were provided during the first half of calendar year 1972.

**Log of Fabrication of 152-cm-Diam (60-in.) Primary Mirror  
(8 March through 16 December 1971)**

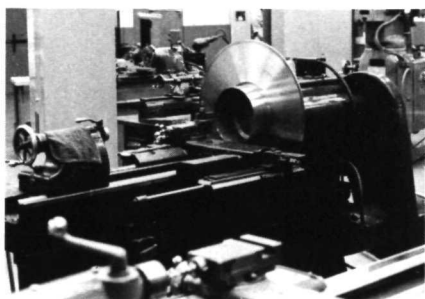
8-17 Mar.	183-cm-diam (72-in.) CER-VIT blank edged to 152-cm diam.
17-29 Mar.	18-cm-diam (7-in.) central hole cut out.
29 Mar.-5 Apr.	Mirror curvature generated by diamond wheel.
5-19 Apr.	Central hole enlarged to 30.5-cm diam (12-in.)
19-26 Apr.	Rough grind starting with 80 grit through 180, 220 to F-l.
26 Apr.-3 May	Blank turned over and recentered, and back curvature generated by diamond wheel.
3-21 May	Vacation period.
24 May	Back flat surface ground with 30 $\mu$ m, 12 $\mu$ m, and 3 $\mu$ m grit.
25 May	Made polishing tool for back flat surface.
26-27 May	Polished back flat surface.
28 May	Cleaned up and prepared to move to 152-cm machine.
1-2 June	Ground stainless-steel support.
3 June	Moved blank to 152-cm machine.
3-7 June	Unsuccessful attempt to room-temperature-vulcanize (RTV) bond primary to support.
7-9 June	Bead-sealed hub, successful RTV bond, centered blank on table for final fine grind.
11 June	Started grind with 30- $\mu$ m grit.
14 June	Finished grind with 12- and 3- $\mu$ m grit.
15 June	Made pitch lap and put to press.
16 June	First polishing run.
16-18 June	Polished blank spherical with 122-cm-diam (48-in.) lap weighing 222 kg (490 lb) (15 h total).
21 June	Made 56-cm-diam (17.5-in.) lap weighing 14 kg (31 lb) and put to press.
22 June	Started polishing to obtain final parabola.
22 June-3 Aug.	Polishing and testing by visual knife-edge test.
3 Aug.	First knife-edge test graph plotted. Polishing continued.
10 Aug.	First use of Shack's test method. Polishing continued.
10 Sept.	Photographic null testing initiated. Zonal polishing initiated.
11 Oct.	Last polishing run. Testing continued.
2 Nov.	Finished testing primary.
9 Nov.	Primary taken to Kitt Peak mountain for aluminizing.
22 Nov.	Mirror taken from Kitt Peak to Mt. Lemmon.
16 Dec.	Telescope put into approximate collimation.



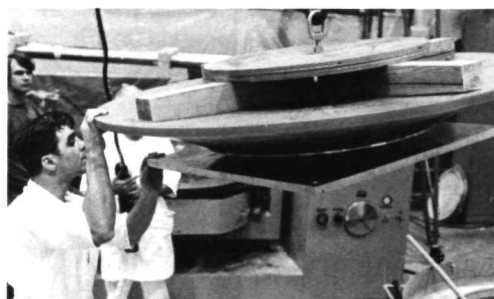
A. Annulus removed in edging the primary.



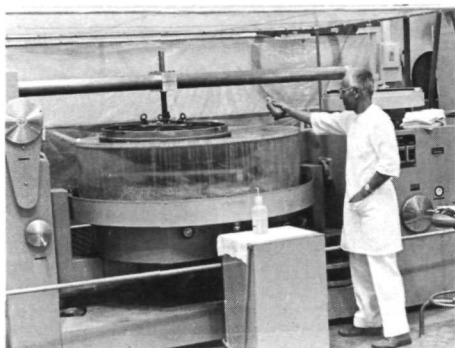
B. Transporting primary to polishing machine after the curve on the back had been generated.



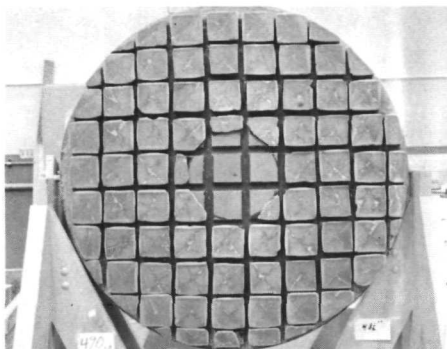
C. Mirror mount being machined.



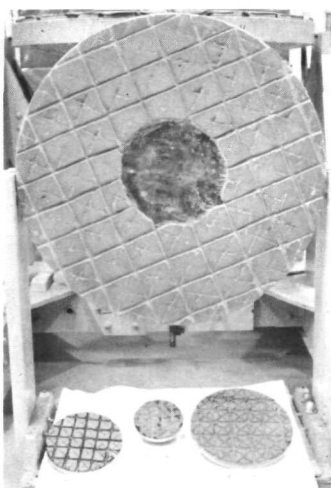
D. Loading mirror with mount onto polishing machine. Center and edge thicknesses of mirror can be seen.



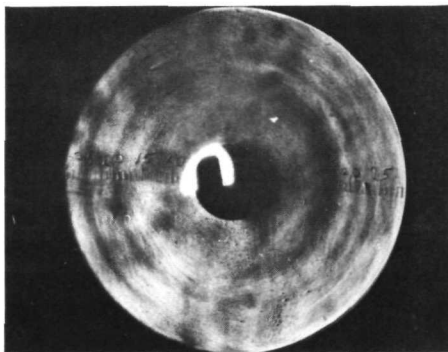
E. Polishing the primary.



F. 48.5-in.-diam. tool weighing 490 lb used for the initial polishing of the primary.



G. Tools: 6 in. and 3.5 lb, 9 in. and 5 lb, 12 in. and 10 lb, 36 in. and 165 lb used for figuring the primary.



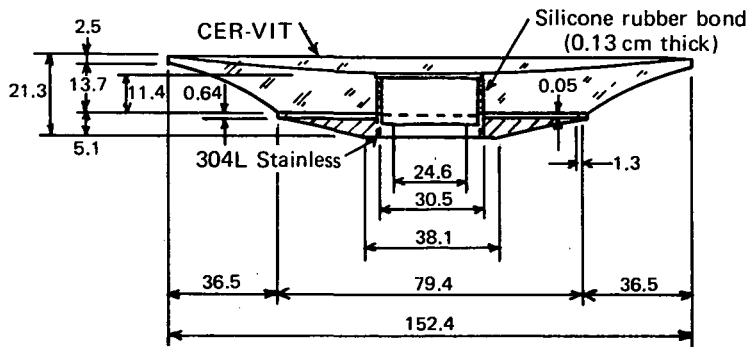
H. Null lens test photograph taken near completion of figuring shows a smooth finish with residual symmetrical zones.

# PRIMARY MIRROR BLANK SHAPE AND MOUNT DESIGN

The following quote is from an article<sup>1</sup> by W. E. Carter. To avoid duplication with other sections of this report, some parts have been omitted.

The gift of a 183-cm diam, 16.5-cm thick Cer-Vit blank by the Optical Sciences Center, University of Arizona, provided an opportunity to construct a glass replacement mirror for the existing metal mirror at a minimum cost. The blank was undesirable for use as a traditional telescope primary mirror for several reasons: The ratio of diameter to thickness was approximately 11, as compared to the usually desired 6. An area of air inclusion, referred to as roping, was visible near the center of the blank. Three cracks, approximately 10 cm in length and 1 cm deep (caused by a previous testing program), were present at the edge. The AFCRL telescope could not accommodate the weight of a traditional primary—a lightweight, center mount design compatible with the existing telescope frame was required. Fortunately, a blank of the same general size and shape as the discarded metal primary could be generated such that the defects in the original blank would be removed during the sizing and shaping operations.

A 2.5-cm edge thickness was chosen, and the sectional depth required to maintain a uniform stress on the figured surface (when oriented horizontally) was computed at each 0.25-mm increment of radius. The limiting depth of the blank, 16.5 cm, was reached at a radius of 39 cm. An interfacing between the glass and the telescope backplate, which would provide additional structural support for the mirror and facilitate mounting, was required. The figure below details the author's design.



AFCRL 152-cm  $f/2.5$  mirror. Design credit: W. E. Carter.

The glass is supported by a 79-cm diam stainless steel mounting plate. The mounting plate is 5 cm thick over the central 38-cm diam and then tapers to an edge thickness of 0.6 cm. An optically ground 1.3-cm wide seat supports the glass along the plate's circumference. The central portion of the back of the glass blank was optically ground and polished flat. The junction between the glass and steel cannot transfer significant shear forces, and radial displacements of the two materials caused by temperature variations and orientation related gravitational loading should have no effect on the figured surface. An 11-cm long 30-cm diam, stainless steel tube with 0.5-cm wall thickness was shrunk fit into the mounting plate, and the glass was bonded to this tube with RTV silicone rubber (Dow Corning type 93-046 catalyst cured). The rubber bond is 0.05 cm thick and was injected between the support tube and the glass through a series of grease fittings. Tapped holes in the back of the mounting plate allow the mirror assembly to be bolted directly to the telescope backplate.

Extensive testing of the mirror under varied operating conditions indicates that the design is highly satisfactory. We believe the use of this mount design will afford a significant savings in the construction costs of moderate aperture, astronomical quality telescopes in the future.

An interesting modification to the design, not mentioned in Carter's article, was the addition of six screws in the telescope backplate that could be turned to bring pressure on the stainless-steel mounting plate around its circumference. These were put in as insurance against either the presence of astigmatism in the finished mirror due to mount-blank warpage or, less likely, insufficient time to obtain the desired mirror figure. In other words, we were anticipating the need for slight corrections to the mirror figure after the mirror had been installed in the telescope. Shop tests indicated that these adjustable screws would probably suffice.

In fact, it turned out that the mirror maintained its excellent figure after mounting in the telescope and that the figure was independent of the telescope pointing angle. However, a disconcerting observation was made in the first photographs of the moon—a double image was obtained. At first we thought the second image originated in the multielement relay optics. One by one the various possibilities were eliminated until no likely ones remained. At this point Carter turned the adjusting screws until they were just making contact with the stainless-steel mount; the second image disappeared. The telescope drive motor, which drives the telescope at a rate of 25 steps per sec, evidently caused a resonant vibration in the mirror mount that was readily damped out by the adjusting screws. Needless to say, this was an entirely unpredicted use for the adjusting screws.

## OPTICAL DESIGN

### *Telescope Optics*

To be compatible with the existing fixtures of the AFCRL telescope, the replacement mirrors were defined as follows:

Primary: 152-cm (60-in.) diam,  $f/2.5$ , CER-VIT  
Secondary: 41-cm (16-in.) diam, final speed  $f/8$ , CER-VIT  
Mirror separation: 285.7 cm (112.5 in.)  
Focus: 304.8 cm (120 in.) from secondary  
Field of view: greater than  $\pm 0.25^\circ$ .

The Ritchey-Chrétien aspheric formulation was selected because of the requirement that full-field tracking should provide adequate resolution for the viewer and the image dissector guidance unit. This type of telescope has a residual astigmatism of only 1 arc sec at full field whereas the simpler inverted Dall-Kirkham (with spherical primary mirror and elliptical secondary) has 14 arc sec of tangential coma at full field. It was felt that the additional fabrication difficulty was justified because it greatly simplified the design of the tracker optics.

The aspheric surface has a profile given by

$$\text{Sagitta} = \frac{y^2}{R + [R^2 - (K + 1)y^2]^{1/2}}$$

where  $R$  is the design radius of curvature,  $y$  is the zonal radius distance from the center line, and  $K$  is a number that describes a conic surface, being zero for a sphere,  $-1$  for a paraboloid, or other values to describe any other conic of revolution. Both mirrors are conics rather than general aspherics. Exact ray targets defining marginal spherical aberration and full-field coma were corrected with the ACCOS computer program. Residual coma and spherical aberration were well under 1 arc sec.

The initial prescription was

Primary  $R = 762$  cm (300 in.),  $K = -1.0658$   
Secondary  $R = 275$  cm (109.09 in.),  $K = -4.4553$ .



### *Test Optics*

The designer and optician worked closely on this project. To minimize fabrication time and to ensure optimum optical performance, the designer allowed the optician unusually loose tolerances on the radii, and the optician accepted revised aspheric prescriptions as the work progressed. After generation of the surfaces, the curvature of the primary was too strong; therefore, we computed new test values to restore exact correction.

The final prescription was

Primary  $R = 759.6$  cm (299.05 in.),  $K = -1.0659$

Secondary  $R = 275$  cm (109.09 in.),  $K = -4.4449$

Mirror separation = 284.5 cm (112.0 in.)

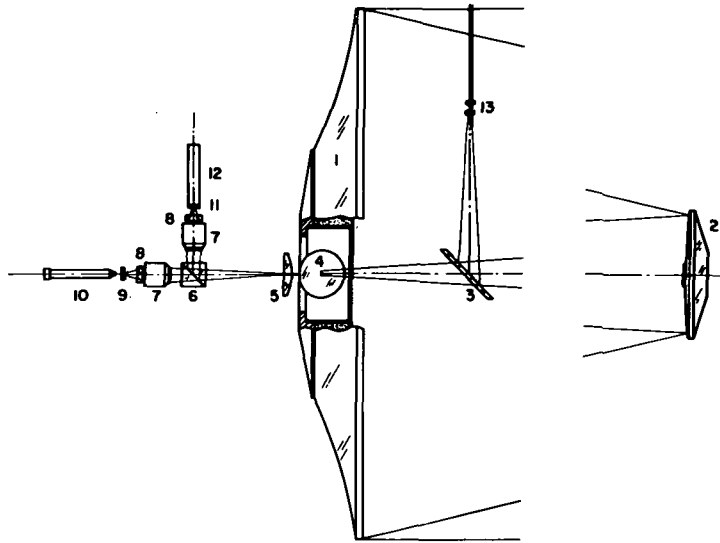
Back focal distance = 305.4 cm (120.26 in.).

The progress of the primary was optically monitored with an Offner null lens system.<sup>2</sup> This consisted of a small field lens and a large single-relay lens. With the final measured radii, thicknesses, and melt data for the optical glass, the Offner system had a theoretical error of  $0.01\lambda$ . Normal use was with filtered mercury light at 546.1 nm; computed respacings enabled it to be used with 632.8-nm laser light for interferometric testing near the conclusion of fabrication. A detailed discussion and prescription for the null lenses is beyond the scope of this report.

The secondary mirror was tested in the Hindle test, and the appropriate conjugates were calculated and given to the opticians. The Hindle test, in which a spherical concentric mirror is used, is a perfect null test and is free of chromatic effects.

### *Laser Channel*

The 152-cm-diam telescope is a multichannel device. First, it transmits a 152-cm-diam collimated beam of pulsed ruby light (694.3 nm) toward the moon. Second, it receives some minute fraction of this light after reflection from corner cube arrays left on the moon by astronauts. Both the transmission and reception of this beam are accomplished with the beam diverted  $90^\circ$  from the flat plate (see figure on p. 14, item 3). The central area of this 1.27-cm ( $\frac{1}{2}$ -in.)-thick piece of optical-quality fused silica is corrected for flatness and given a precision polish. It is coated with a dielectric film that passes much of the visible light and reflects 99% of the pulsed ruby 694.3-nm radiation. The laser interfacing lenses cause the laser to appear to emerge from a point at the focus of the 152-cm-diam telescope. Focusing is done by moving the secondary mirror and verifying the collimation by placing a small hand monocular at lens 13; if a star is focused, then the transmitted beam will be focused. The use of CER-VIT mirrors and a quartz beamsplitter helps maintain focus during operation although frequent checks on focus are required.



152-cm diam telescope. (1) 152-cm  $f/2.5$  hyperboloid CER-VIT primary mirror. (2) 40-cm hyperboloid CER-VIT secondary mirror. (3)  $23 \times 15$ -cm elliptical dichroic beamsplitter (99% reflectivity at 694.3 nm). (4)  $23 \times 15$ -cm elliptical compensator plate. (5) 14-cm field lens. (6) 76-mm dichroic cube beamsplitter. (7) Nikkor-H 35-mm  $f/1.8$  camera lens and portrait attachment. (8) Spherical aberration corrector plate. (9) Field flattener and reference reticle. (10) 40X microscope on X-Y stage. (11) Field flattener bonded to face of image dissector tube. (12) ITT F4011 image dissector tube. (13) Laser interfacing lenses.

### *Tracker Optics*

The tracker has two channels. One channel contains a 2.54-cm-diam image dissector that is used to fix onto some feature on the surface of the moon and to guide the telescope automatically. Fortunately, the image dissector will lock onto the centroid of even a poorly defined detail caused by aberration or other effects, so its pointing sensitivity is a good deal greater than its resolution. The image dissector channel differs from the offset-guiding/setting channel in that a dichroic film directs blue-green light into it whereas the other channel gets principally yellow-red light. Its field flattening lens is cemented directly to the image dissector tube to eliminate probable ghost images that would occur otherwise (two plane-parallel surfaces near a focus usually cause this). See p. 17 for a detailed description of the tracker optics.

The image dissector tube defined the reduction required in the relay system. To form a  $0.5^\circ$ -diam image of the moon onto a 2.54-cm-diam surface, we needed a 152-cm-diam telescope having an aperture ratio of  $f/1.9$ . A quality specification of a few arc sec resolution had to be carefully weighed against the cost of designing a special optical system allowing this degree of correction. Because of the nature of the image dissector tube and because of the filtering occurring naturally (the beamsplitting plate for the laser automatically strips the spectrum of ruby red whereas the glass cube is dichroic), we felt that perhaps ordinary photographic lenses plus additional simple lenses could be incorporated into an inexpensive yet adequate transfer system.

The design requirements then were based on the designer's familiarity with photographic lenses. We desired to keep the apparent field of view small because photographic lenses have limiting field defects that should be avoided. However, the focal length could not be excessive. We concluded that a focal length of 85 mm would permit a  $\pm 7^\circ$  field of view and would also minimize the defects of auxiliary lens attachments. A field lens with a clear aperture of 13.3 cm (5¼ in.) that would allow a maximum real field of 36 arc min was mandatory. This would cause the light from the telescope to enter the small (approximately 4.8-cm (1.9-in.)) pupil of the photographic lens. The photographic lens was supplemented with a portrait attachment (technically, a collimator). To eliminate the spherical aberration caused by this portrait attachment, a 1.85-cm (¾-in.) slab of glass was placed in the fast ( $f/1.9$ ) convergent beam from the photographic lens. Because the dominant field curvature of the telescope-plus-field-lens-and-portrait-attachment was inward curving, we added a plano-concave field flattener at the end of the train. The image dissector channel would have been useless without a field flattener, and the visual channel would have been inconvenient in operation.

Cost was of paramount concern; thus we compromised as much as possible. Both field lens and portrait attachment were plano-convex and had the same radius of curvature. Some improvement would have been optically obtained by allowing meniscus shapes, but these would be more costly. Chromatic aberration was disregarded because its correction would have involved the use of more lenses. All curvatures were made to fit existing test plate radii, thereby allowing a further reduction in cost. Although the designer specified comparatively loose tolerances, the optician insisted on maintaining pride in workmanship. We do not know what precisely would have happened had the original photographic quality tolerances been applied on the attachments. In the visual train, there were 15 lenses or flat transmitting and reflecting optics and approximately 28 air-glass surfaces not including the microscope used to view the image. Despite the enormous number of sources of probable error, the maximum extent of the spread function observed by the designer appeared to be within 2 arc sec on axis, with the nucleus of the energy concentrated in an area a little below this. This speaks well for the usefulness of commercial optical surfaces.

### *Further Design Considerations*

We cannot simply patch up a photographic lens to serve as a finite-conjugate relay because there are field aberrations left as residuals in the design of the portrait

attachment, plate, and field flattener. Although we do not have the optical design for the Nikkor lens, it appears likely that the only major residual aberration will be coma caused mainly by the glass plate. However, coma affects resolution very slightly, and the glass plate eliminates astigmatism, giving a good flat field both on the image dissector faceplate and in the visual guider. Experience to date with the finished telescope suggests that the effectiveness of the image dissector has not been impaired by this residual aberration because most of the viewing is done in the central field where the coma has not been observed. We conclude that the necessary tradeoffs in quality have proved correct.

The tilted 1.2-cm-thick beamsplitting plate used to divert the laser into the 152-cm-diam telescope causes axial aberration in the tracker optics. Used alone, it gives 3 arc sec of axial astigmatism. It is corrected with another plate optically identical to the first, which is tipped the same amount but turned  $90^\circ$  on the centerline. Thus astigmatism is eliminated, and there is slightly less than 1 arc sec of axial coma. Lateral color is tolerable owing to the narrow spectral passband of each channel in the tracker.

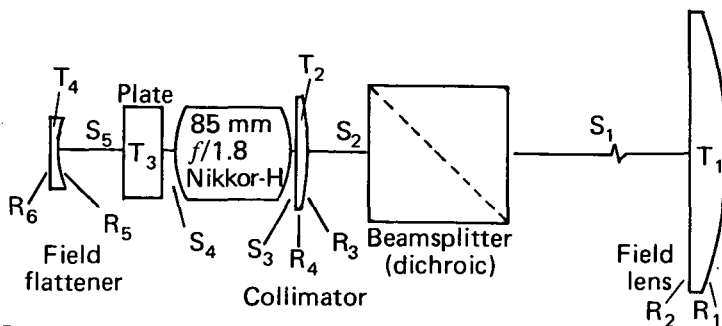
It is not practical to compute distortion because we know too little about the Nikkor lens. Owing to the large number of other lenses and tipped plates, it is necessary to calibrate the distortion of the image empirically; the Pleiades star field is suited for this purpose. A word of caution is that we should not assume coaxial symmetry in the distortion calibration.

The laser is aligned with the axis of the tracker by observing the laser reflection off the corner cube attached to the spider vane (secondary holder vane) in the tracker visual field. The corner cube is nothing more than an autocollimating flat; we observe a 6-arc-sec image of the pulse (diffraction limited in the case of this telescope) in the eyepiece. The  $45^\circ$  flat is adjusted in tilt (two adjustments) until it lines up with the fixed reticle in the guider eyepiece. By definition, the two axes are aligned. Absolute perfection is not required because alignment error can be included in the offsetting calculations.

Ghost images have not been observed when we view the moon or stars, but a displaced (sideways) ghost was once observed when we viewed the laser pulses. This apparently was caused by a chance good alignment of the spider's corner cube in which the flat entrance surface managed to get a direct ghost return to the telescope. We conclude that the corner cubes should be deliberately cocked.

In order to obtain high reflectivity at the laser operating wavelength (694.3 nm), the secondary mirror was gold coated. To minimize handling risk and to expedite delivery, the primary was aluminized at the coating facility operated by Kitt Peak National Observatory.

## Tracker Optics



## Optical Description

Field lens: Plano-convex,  $R_1 = 22.395$  cm (8.817 in.),  $R_2 =$  plane,  $T_1 = 2.54$  cm. Glass SK4 (Schott). Diameter = 13.97 cm (5.5 in.), clear aperture = 13.335 (5.25 in.).

Beamsplitter: 8 cm (3.14 in.). Glass BK7. Special coating to give image dissector green-blue light.

Collimating lens: Plano-convex,  $R_3 = 22.396$  cm (8.817 in.),  $R_4 =$  plane,  $T_2 = 0.635$  cm (0.25 in.). Glass SK4 (Schott). Diameter = 5.08 cm (2.0 in.), clear aperture = 4.724 cm (1.86 in.) minimum.

Nikkor-H: 85 mm,  $f/1.8$ , Code 111021. Operated at an effective field angle of approximately  $\pm 7^\circ$  at  $f/1.9$ .

Plate: Plane-parallel,  $T_3 = 1.905$  cm (0.75 in.). Glass Bausch and Lomb EDF3 (or Schott SF18). Diameter = 4.572 cm (1.8 in.).

Field flattener: Plano-concave,  $R_5 = 9.857$  cm (3.881 in.),  $R_6 =$  plane,  $T_4 = 0.254$  cm (0.10 in.). Glass SK4 (Schott). Diameter = 3.175 cm (1.25 in.), clear aperture = 2.857 cm (1.125 in.) minimum.

## Tracker Assembly Notes

### 1. Spacings

- Field lens: The front surface of the field lens is nominally at the cassegrainian focus of the 152-cm telescope.
- Beamsplitter: Spaces  $S_1$  and  $S_2$  may be selected at will, but their sum will be approximately 28.803 cm (11.34 in.).
- Collimating lens:  $S_3$  should be as small as possible, but it is an afocal space and therefore not significant in affecting the other spacings. In the AFCRL assembly the collimating lens is attached directly to the Nikkor lens.
- Nikkor 85 mm  $f/1.8$ : A very high quality lens is required for good final image quality, and the Nikkor serves this purpose. Other similar lenses may also serve. Because this lens sees collimated light, its length does not affect other spacings. The vertex thickness of this lens is 6.17 cm (2.43 in.).
- Plate: The sum of  $S_4$  and  $S_5$  will be approximately 3.048 cm (1.20 in.), and the position of the plate has no effect optically.
- Field flattener: The final image falls on  $R_6$ . This may be accomplished with the focusing ring on the Nikkor lens.

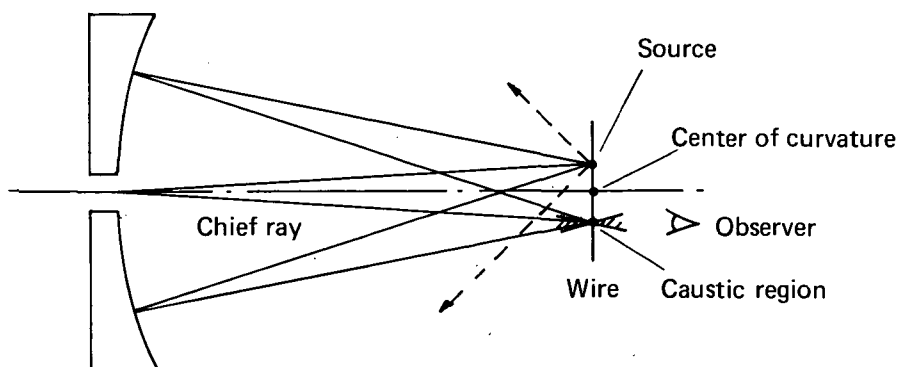
2. Antireflection coatings: Because of the large number of surfaces, all optical elements are anti-reflection coated. Field lenses should be given high-efficiency coatings to avoid ghost images. The use of high-index glass enables us to use magnesium fluoride on the remainder.

3. Collimation: Relies on accurate design and fabrication of mechanical assemblies. No problems encountered.

## QUANTITATIVE WIRE TEST ANALYSIS

### *Theory*

In the axial wire test, a vertical wire is inserted in the caustic region of the return beam when the mirror is illuminated by a point source near the center of curvature of the mirror (see the figure below). An eye placed behind the wire will see a shadow projected onto the mirror for all rays blocked by the wire. If the mirror is a true conic of revolution, the caustic will be a figure of revolution about the chief ray. If the wire is positioned laterally to intersect the chief ray, the shadow will consist of a vertical straight line parallel to the wire and centered on the mirror. In addition, a circular shadow will also be produced that will be centered on the mirror. The circular shadow identifies the zone from which the reflected rays will intersect the chief ray at the location of the wire. As the wire is moved axially, the radius of the circle will vary. If the point source and the wire are located in the same plane and move together, the axial position of the wire as a function of the radius of the circle will map the axial portion of the *caustic of the normals* to the mirror surface. From this information, a profile of the departure of the actual mirror surface from the desired conic can be determined.



Schematic of axial wire test.

The properties of the axial caustic of the normals to a conic surface of revolution are remarkably simple. Because the system is rotationally symmetrical about the axis of revolution, we need consider the problem in only two dimensions in a meridional plane.

Let the axis of revolution coincide with the  $z$  axis. Then  $z = z(y)$  will represent the meridional section of the conic of revolution. Explicitly it is given by

$$z(y) = \frac{y^2/R_0}{1 + [1 - (K + 1)(y/R_0)^2]^{1/2}} \quad (1)$$

where  $R_0$  is the paraxial radius of curvature and  $K = -\epsilon^2$  is the conic constant for a conic of eccentricity  $\epsilon$ . For a sphere  $K = 0$ , and for a paraboloid  $K = -1$ . If  $K < -1$  the surface is a hyperboloid, and if  $-1 < K < 0$  it is a prolate ellipsoid. If  $K > 0$  the surface is an oblate ellipsoid.

If the distance from the mirror vertex to the intersection of the surface normal with the axis is represented by  $l$ , then it can be shown that

$$\begin{aligned} l - R_0 &= -Kz(y) && (\text{exact}) \\ &\approx \frac{-K}{2R_0} y^2 - \frac{K(K+1)}{8R_0^2} y^4 && (\text{approximate}). \end{aligned} \quad (2)$$

Moreover, the length  $R$  of the normal from the surface to its intersection with the axis is determined by

$$R^2 = R_0^2 - Ky^2 \quad (\text{exact}). \quad (3)$$

If the actual surface departs from the desired conic by an amount  $s(y)$ , then the axial intercepts of the surface normals will depart from those determined by the above equations by an amount  $\Delta l(y)$ . It can be shown that the surface departures,  $s$ , can be determined approximately by

$$s \approx -R_0^{-2} \int y \Delta l dy + s_0. \quad (4)$$

The quantity  $s_0$  is an arbitrary constant of integration. This approximation is valid if (a)  $\Delta l \ll R_0$ ; (b)  $s \ll \Delta l$ ; and (c)  $(K + 1)y^2 \ll R_0^2$ . Item (c) is valid if  $y \ll R_0$  (large  $f$ -number) or if  $K \approx -1$  for any  $f$ -number. These conditions are adequately met in the present case.

In the implementation of the test, the value of  $K$  is given by the optical designer. Because the mirror has a central hole, the value of  $R_0$  is obtained by measuring  $R$  for some zone radius  $y$  and then using Eq. (3).

The values of  $\Delta l$  are determined as follows. Let  $l' = l + \Delta l$  represent the actual axial intercepts whereas  $l$  represents the ideal. Then, as a function of  $y$ , the wire test determines values of  $w(y) = l'(y) - l'(y_{\text{ref}})$ , where  $y_{\text{ref}}$  is an arbitrary reference

zone. In the present case, the 15.2-cm (6-in.) zone was chosen. Then

$$\Delta l(y) = w(y) - [l(y) - l(y_{\text{ref}})] + \Delta l(y_{\text{ref}}). \quad (5)$$

The quantity  $w(y)$  is the difference between the axial setting for each zone  $y$  and the axial setting for the reference zone  $y_{\text{ref}}$ . The quantity  $l(y) - l(y_{\text{ref}})$  can be calculated from Eq. (2). The quantity  $\Delta l(y_{\text{ref}})$  is undetermined, but its value, which is small, is a constant for all  $y$ .

The values of  $s$  are then obtained by the integration indicated in Eq. (4). The effect of the undetermined constant  $\Delta l(y_{\text{ref}})$  is to introduce a parabolic component,

$$s' = \frac{\Delta l(y_{\text{ref}})}{2R_0^2} y^2, \quad (6)$$

to  $s$ . Small changes in  $s'$  correspond to changes in  $R_0$  that are smaller than can be measured directly. Therefore, an arbitrary value can be assigned to  $\Delta l(y_{\text{ref}})$  to flatten appropriately the  $s$  curve representing the departure of the actual surface from the ideal surface. In addition, the value of  $s_0$  in Eq. (4) can also be assigned arbitrarily, which corresponds to choosing different reference levels in the vicinity of the surface of the mirror.

One particular application of the otherwise arbitrary choice of  $\Delta l(y_{\text{ref}})$  and  $s_0$  is the coordination of a given test run with the preceding one if an appreciable portion of the mirror remains untouched between the two test runs. Values of the two constants are chosen to bring into coincidence the  $s$ -curve profile of the second test with that of the first in the untouched region. The remaining difference between the curves then shows how much glass has been removed.

### *Application*

To make data reduction practical for the optical shop, an appropriate program was prepared for a Hewlett-Packard 9100B calculator attached to a 9125A plotter. Two sequential entries of the data were required. In the first entry the arbitrary constants were made zero, and the values of  $s$  were plotted against  $y^2$ . In this type of plot a straight line corresponds to a parabola in the conventional  $s$  versus  $y$  plot. An appropriate straight line for correcting the data was selected, both constants were determined, and their values were entered into the calculator. The second data entry produced a conventional  $s$  versus  $y$  plot of the corrected data. The process took approximately 10 min, thereby making the procedure quite practical for the optical shop.

The following table and set of graphs show how the method worked in practice. The table lists the polishing parameters as noted by the optician on a



daily basis. The numbers in the left-hand column correspond to the numbers on the graphs that follow. At the end of the run time listed in the right-hand column the curve was plotted. From studying the table and graphs the reader can quickly appreciate the strategy used for achieving the desired figure in the least time. This approach dramatically reduces the chance of overshooting in polishing a particular zone—a condition that can be very time consuming to correct.

Curve number	Test date	Tool size (in.)	Approximate weight on tool (lb)	Zone (in.)	Stroke (in.)	Offset (in.)	Run time (h)
2	8-10-71	17½	31	26	9	13	30*
3	8-13-71	17½	20	8 to 23	6	8½ to 10	18*
4	8-17-71	9	10	9 to 23	6	8½ to 10	13†
	8-19-71	17½	40	7 to 23	6½	8½ to 10	13†
5	8-19-71	17½	40	7 to 23	6	10 to 12	6†
	8-20-71	17½	38	8 to 14	5	12½	5†
	8-23-71	12	15	9 to 11	5	13½ to 15½	5†
6	8-24-71	12	15	9 to 12	5	9½	4†
	8-25-71	9	15	9 to 12	5	9½	7†
7	8-26-71	9	10	8 to 11	5	9½ to 11	4†
	8-27-71	9	10	9	5½	9½ to 11	8†
8	8-30-71	6	10	8 to 9	5½	9 to 11	5†
	8-31-71	6	10	8 to 9	5½	9 to 11	8†
9	9-01-71	6	10	8 to 9	2	7 to 9	3†
	9-02-71	6	10	8 to 9	2	7 to 9	3†
10	9-02-71	17½	40	28	1	19	1†
11	9-03-71	6	10	7 to 10	4	9 to 11	8†
	9-07-71	6	10	8	2	7	2†
	9-07-71	4	5	8	2	7	2†
12	9-07-71	4	5	29	¾	27	3†
	9-08-71	4	5	29	½	28	3†
13	9-10-71	4	5	29	½	28	1†
	9-10-71	6	5	13½ to 15	2¼	14	1†
	9-13-71	4	5	24	½	29	0:30†
	9-13-71	4	5	29 to 30	¼	29	0:30†
	9-14-71	4	5	24 to 25	¼	29	1†
	9-14-71	4	5	29 to 30	¼	29	1†
	9-15-71	17½	40	6 to 20	7	7 to 19	4†
	9-16-71	17½	40	8	7	7 to 12	5†
	9-20-71	4	5	25 to 27½	½	24 to 28	3†‡
	9-21-71	4	5	25 to 27½	½	24 to 28	1†
	9-21-71	17½	20	10	2	9 to 13	2†§
	9-22-71	17½	20	26	2½	24½ to 27½	3†
	9-23-71	6	10	29	½	28	3†
	9-24-71	17½	20	10	3	9 to 15	4:30†
	9-27-71	17½	20	10	3	9 to 15	4:30†
	9-28-71	12	10	22	2	19½ to 22½	2†§
	9-28-71	6	10	22	½ to 1½	19½ to 22½	1†
	9-29-71	17½	20	22	½	19½ to 23	1†
14	9-30-71	9	0		½	22 to 24	1†
	10-04-71	4	5	20	1	19½ to 21	1†
	10-04-71	6	10	20	1	19½ to 21	1†
	10-05-71	9	10	20	1	19½ to 21	1†
15	10-05-71	6	5	8½	1	8 to 9	1†
	10-06-71	4	5	19	½	19 to 19 ¾	0:40†
16	10-06-71	4	10	19	½	19 to 19 ¾	0:40†
	10-07-71	4	10	8 to 9½	½	8 to 9½	0:20†
	10-07-71	4	10	18½	½	18 to 19	0:20†
	10-08-71	4	10	8 to 9	½	18 to 19	0:14†
	10-08-71	4	10	17 to 18	½	18 to 19	0:10†
	10-08-71	4	10	23½ to 24½	½	18 to 19	0:05†
17	10-08-71	4	10	28	½	18 to 19	0:04†
	10-11-71	4	10	10	1	9½ to 10½	0:20†
18	10-11-71	6	10	10	1	9½ to 10½	0:20†

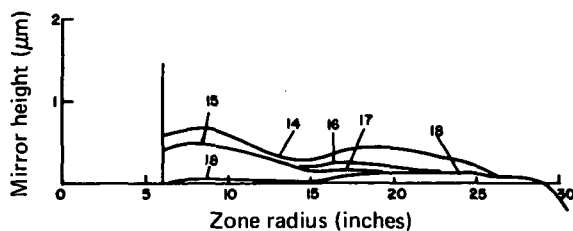
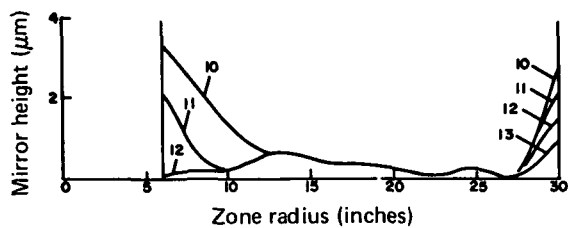
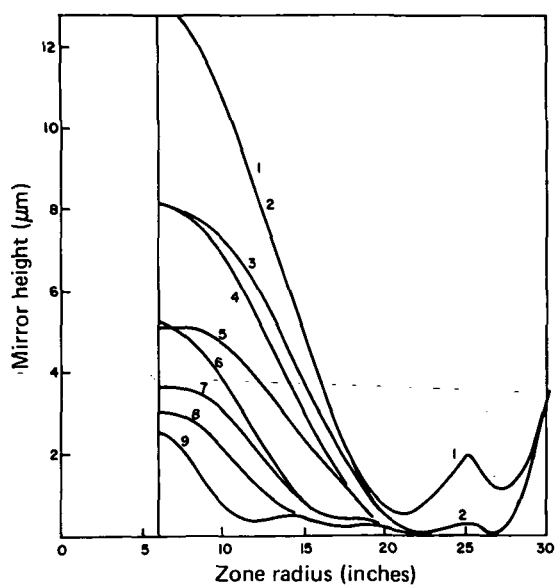
\* Speed and direction of tool varied each ½ h and offset moved back and forth each ½ h.

† Tool turned continuously by hand and offset adjusted without break in continuity.

‡ One 2-h run and one 1-h run.

§ Two 1-h runs.

|| Three 1-h runs.



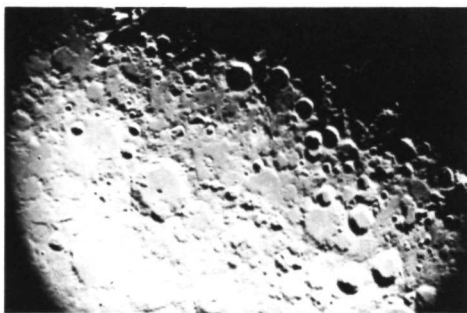
Mirror surface profiles. (Note: scale has been changed in third graph to show curves more clearly.)

## OPERATIONAL TEST RESULTS

In addition to the shop tests carried out on the primary and secondary separately, some tests were carried out on the combination as an operational system. Micrometer measurements of double star separations indicated resolutions on the order of 0.5 arc sec or about a factor of four better than called for by the specifications. The telescope performance was so well within specifications and the lunar laser ranging time was at such a premium (the telescope was dismantled in June 1972 and transported elsewhere by the United States Air Force) that further quantitative tests were curtailed.

The following is extracted from an article<sup>3</sup> by W. E. Carter on the operational tests of the telescope.

The picture below is a photograph taken by the author at approximately 1100 U.T., 7 January 1972. The view covers a portion of the moon from latitudes 0° to 35° south and longitudes 5° west to 15° east. The field represented by the latitude coverage is approximately 8.5 min of arc. The photograph was taken with a 35-mm camera on Plus X film, with an exposure time of 1/30 of a sec, utilizing the full 147-cm aperture. The inherently high contrast of the negative was somewhat subdued by G. Kew, photographer, University of Arizona's Optical Sciences Center, during printing. Lunar features smaller than 2 km are clearly discernible on the photograph. Observers were able to resolve lunar features of less than one-half that size. The implied resolution has been confirmed by observations of several double stars of known separation, as well as Saturn's ring structure.



Lunar photograph by W. E. Carter.

Of particular significance is the fact that the previously described observations were made during the winter period, with temperatures in the 0 to  $-10^{\circ}\text{C}$  range. The mirror was assembled (i.e., the glass and metal were bonded together) and figured at approximately  $22^{\circ}\text{C}$ . The tests indicate that temperature changes of  $20\text{--}30^{\circ}\text{C}$  are tolerated by the design without significant distortion of the figured surface.

The initial tests must be considered an unqualified success. Long-term stability, critically important to the validity of the design, has yet to be demonstrated; but the manufacture, installation, and initial performance test of the telescope have been successfully completed without major difficulties.

We should add two comments to the above article extract. First, the primary mirror is 152 cm in diameter; the 147 cm referred to arises because a zone 2.5 cm in width was masked off to eliminate image degradation from the turned-down edge. It is our opinion that trying to maintain an excellent figure out to the edge of the blank of a telescope mirror is not a cost-effective procedure and that it is better to start with a blank slightly larger than the required mirror surface and mask off the turned-down edge.

Second, five months after the photograph cited in Carter's article was obtained and immediately preceding the dismantling of the telescope no degradation in the image-forming characteristics of the telescope was detected. This has increased our confidence in the long-term stability of this novel design of astronomical telescope.

## REFERENCES

- <sup>1</sup>W. E. Carter, "Lightweight center-mounted 152-cm  $f/2.5$  CER-VIT mirror," Appl. Opt. 11(2):467-468, 1972.
- <sup>2</sup>Abe Offner, "A null corrector for paraboloidal mirrors," Appl. Opt. 2(2):153-155, 1963.
- <sup>3</sup>W. E. Carter, "Operational tests of the AFCRL 152-cm telescope," Appl. Opt. 11(7):1651-1652, 1972.

KSS

